

## Problems of Planetology, Cosmochemistry and Meteoritica

**Dubinsky A.Yu., Popel S.I. On a possible mechanism of light-induced reactions in the lunar regolith** *UDC 523.34—36*

Space Research Institute (IKI) RAS, Russia, Moscow, nfkpb@bk.ru, [popel@iki.rssi.ru](mailto:popel@iki.rssi.ru).

**Abstract.** Near the surface of the Moon, the velocity of a solar wind proton is about 500 km/s, which corresponds to a kinetic energy of  $\sim 1$  keV. This energy is sufficient for the penetration of a proton into the matter of the lunar regolith, also for multiple rupture of interatomic bonds in it, and for the formation of a hydroxyl group  $-OH$  as well. In particular,  $Si-O-Si$  molecular fragments, which are characteristic for the minerals that form the lunar regolith, are subjected to rupture, so that reactions can occur that cannot be started only by the thermal energy. So, if metal sulfides (for example,  $Ag_2S$ ,  $FeS$ ) are present in the immediate vicinity of the broken bond, then, due to their atomic similarity, the exchange of oxygen and sulfur atoms is possible, which can lead to further formation of reduced metals, their hydroxides, and also water molecules incorporated into the material of the lunar regolith.

**Keywords:** *Solar wind, lunar regolith, Moon, silicon dioxide, sulfides*

### Introduction

Recent studies based on data from the Lunar Reconnaissance Orbiter have revealed the presence of hydrogen-rich regions in the near-surface segments of the Moon at latitudes greater than  $70^\circ$ . The occurrence of near-surface regions rich in hydrogen can be caused by electrons and protons from the solar wind, which are absorbed by the lunar surface and form chemical compounds containing hydrogen, for example, in the form of hydroxyl groups of lunar regolith particles. This implanted hydrogen can accumulate on the lunar surface by the following mechanism: solar wind protons are absorbed at depths up to  $10^{-5}$  cm; at the end of the proton path, they chemically bond with atoms of the lunar regolith, in particular, with oxygen atoms. As a result, tens of percent of oxygen atoms in areas of the lunar soil interacting with solar wind protons are bound into  $-OH$  hydroxyl groups.

However, the results obtained (Mitrofanov et al., 2010) are often interpreted as if there were the presence of water ice in the near-surface lunar regions. The justification for such an interpretation is important from the point of view of future lunar missions and exploration of the Moon, especially in the sense of low probability of free water existence (i.e., which is not included in the near-surface lunar soil) on the Moon, due to intense evaporation into

atmosphereless space during the daytime and the impossibility of condensation at night. Here, we present a possible mechanism for the formation of water molecules included in near-surface lunar soil.

Measurements in 2020 (Li et al., 2020,) also indicated the presence of  $Fe_2O_3$ , in the polar regions of the Moon. The authors explained the existence of iron(III) oxide in the lunar regolith, at taking into account the oxygen from the Earth's magnetosphere, since it is known that the Moon spends about a quarter of its orbit in the plasma of the magnetotail.

However the participation of  $FeS$  molecules is also possible in the formation of iron oxide. Iron sulfide is considered due to the fact that the electronic structure of outer orbitals of sulfur is similar to oxygen (although it differs from the latter by a large radius), so that the replacement of an oxygen atom by a sulfur atom will not lead to a significant defect in the  $SiO_2$  crystal lattice. Other homologous atoms (Se, Te) are not taken into account even more difficult to integrate into the silicon oxide lattice, and also because of their low content in the lunar regolith.

An approach is proposed according to which an important role for near-surface reactions in the lunar regolith is played by the flux of solar wind protons, whose kinetic energy near the orbits of the Earth and the Moon is on average about 1 keV (which corresponds to a velocity of the order of 300–700 km/s) and makes it possible to break the strongest molecular bonds, involving atoms from the composition of surface minerals. First of all, this concerns oxygen, the most common element that is part of the regolith and is almost completely in a bound state.

### Mechanism of iron(II) oxide formation

Consider the region of the immediate vicinity of iron sulfide and silicon oxide (see e.g., Dubinsky and Popel, 2021).

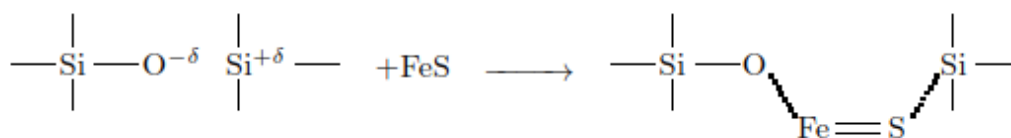
(a) When a solar wind proton passes, the  $Si-O$  bond breaks with the formation of partially charged atoms of  $Si^{+\delta}$  and  $O^{-\delta}$ . The flux density of solar wind particles near the lunar surface is about  $3 \times 10^8 \text{ cm}^{-2} \cdot \text{s}^{-1}$ . The depth of penetration of protons into the regolith is of the order of 10–100 nm (Hapke, 2001), which corresponds in order of magnitude to the number of  $Si-O$  bonds destroyed along the path of  $H^+$ . Thus, assuming that the characteristic distance between atoms in a  $SiO_2$  crystal is about 0.2 nm,



we find that the breaking of 100–200 bonds corresponds to a distance of ~20–40 nm. The proton deceleration time is about  $10^{-13}$  s. In turn, to estimate the number of acts of breaking of Si–O bonds in the near-surface layer of the regolith, we will take the value of 30 nm as the depth of passage of the proton. Then, in this layer with an area of  $1 \text{ cm}^2$  happens

about  $3 \times 10^8 \text{ cm}^{-2} \times 200 = 6 \times 10^{10}$  instances of breaking. Thus, in the near-surface layer ~30 nm thick, we have about  $2 \times 10^{16} \text{ cm}^{-3} \cdot \text{s}^{-1}$  instances of breaking Si–O bonds per unit volume.

(b) At the next stage, an intermediate complex with the FeS molecule is formed.



The FeS molecule is characterized by a pronounced ionization of iron and sulfur atoms. For this reason, there is a tendency to the formation of intermediate bonds Fe–O and S–Si. It should be noted that the complex does not necessarily have a flat structure. It is quite possible that the  $\text{O}^{-\delta}$  atoms

and  $\text{Si}^{+\delta}$ , as well as the FeS molecule lie on crossing lines.

(c) Finally, oxygen captures the iron atom, as a result of which iron (II) oxide is released, and the sulfur atom closes bonds with silicon atoms, replenishing the oxygen left in this position.



The rate of the above-described process is limited by the following factors.

(1) The Si–O bond can be broken down only during the lunar day since it requires a flow of solar-wind protons, which is absent during the lunar night. During a lunar day, the energy of solar-wind protons is insufficient to break the Si–O bond.

(2) It is known that the lunar regolith consists of fragments of lunar rocks and minerals, glasses, lithified breccias, fragments of meteorites, and other substances with a size ranging from nano- and microscale dust particles (which predominate in the size distribution) to objects that are several meters across. For the reactions described above, the diffusion of silver sulfide into the region of particles of the lunar regolith is important. If the characteristic particle size is taken to be  $1 \mu\text{m}$ , the diffusion time is almost 500 s, which is significantly less than the

length of the lunar day (around 14 Earth days). Thus, the contact of silver sulfide with a regolith grain leads to a relatively rapid penetration of  $\text{Ag}_2\text{S}$  into the silicate lattice.

(3) These reactions occur in the regolith layer facing the Sun and have a thickness of around  $10^{-5}$  cm (Starukhina, 2001), which is associated with the need for solar-wind protons to reach the zone of contact with silver sulfide (to break the Si–O bond). An estimate taking into account the characteristic energies of Ag–S and Si–S bonds makes it possible to determine the probability of replacement of an oxygen atom by a sulfur atom around  $10^{-5}$ .

As already mentioned, the Si–O bond energy is about 450 kJ/mol, while a similar Si–S bond is characterized by a bond energy of approximately 265 kJ/mol (Nekrasov, 1973). In turn, the energy of the double bond in the FeS molecule is 322 kJ/mol, and

the same in FeO is 390 kJ/mol (Volkov and Zharsky, 2005).

From this it is possible to estimate the total energy effect of the reaction (4) which consists in the absorption of energy approximately equal to  $\Delta E = 2 \times 450 + 322 - 390 - 2 \times 265 \approx 300$  kJ/mol. It is also required to overcome an energy barrier of the order of the bond breaking energy, i.e. about 400–450 kJ/mol, and thus, direct replacement of oxygen with sulfur requires not only a total energy of about 3 eV for its implementation, but also an initial energy input of about 4–4.5 eV. Obviously, even for daytime lunar temperatures of 400 K, the thermal energy is about  $3.5 \times 10^{-2}$  eV, which makes the direct reaction practically unrealizable.

It should be noted that certain simplifications were made in the calculations. Thus, when operating with Si–O bonds, we use averaged data, assuming that the characteristics of the siloxane bond in silica or, for example, pyroxenes, are equivalent. Also, the standard silicon–sulfur bond energy (in pure SiS<sub>2</sub>) differs from the energy of deformed Si–S–Si bonds in the composition of a silicon-containing mineral. The initially smaller interatomic distance between

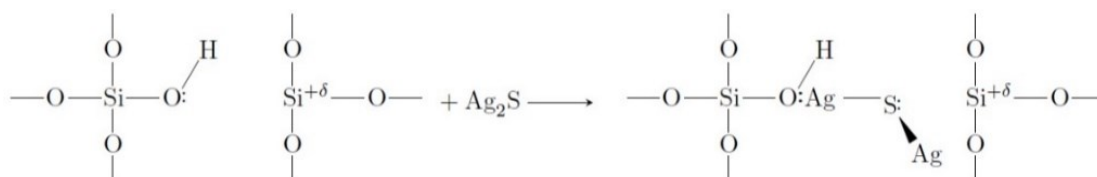
silicon atoms, specified by the Si–O–Si bonds (the length of the Si–O bond is about 0.164 nm), increases due to the appearance of sulfur between the silicon atoms, but the bond angle around the sulfur atom decreases (with the length of the Si–S  $\approx$  0.215 nm (Nekrasov, 1973). Also, the Si–O<sup>δ</sup> bond in an excited state and, accordingly, the energy of this bond, differs from the situation with an unperturbed silicon–oxygen bond. However, the main order of magnitude shows an obvious difference in energy effects, despite some simplifications made in the calculation.

#### Mechanism of water molecule formation

Water molecules can be formed through the following mechanism of exchange by sulfur and oxygen in those areas of the regolith, where silver sulfide and silicon dioxide are in direct contact. (see e.g., Dubinsky and Popel, 2019).

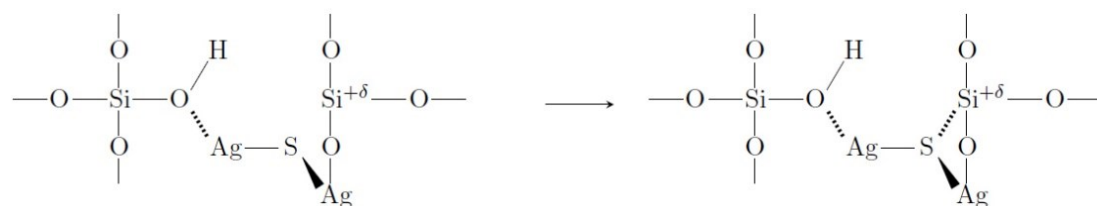
(a) The first light-induced stage is the same as for FeO formation

(b) Next, sulfur and silicon atoms approach; in turn, the silver atom approaches the oxygen atom to form intermediate complex:



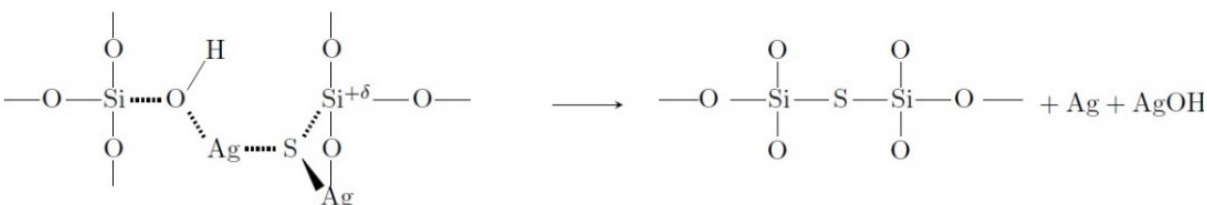
(c) Then, a single intermediate complex is formed due to covalent-hydrogen bonds, and the Ag–

S bond breaks down:



(d) This results in the separation of silver hydroxide and, finally, the separation of the silver

atom.



The amount of water produced by the above-mentioned mechanism can be estimated in the following way. The upper layer of the lunar surface with a thickness of a few centimeters is a regolith evolving from, multiple breakage due to meteoroid hits (Golub', A.P. et al., 2012). Typically, the particle

size of the lunar regolith is several tens of micrometers. Due to hits of meteoroids (including micrometeoroids), the regolith particles are constantly mixed. Since the solar-wind protons are absorbed in lunar regolith particles at depths of up to  $10^{-5}$  cm = 0.1 μm, the chemical processes described

above occur only in a narrow near-surface layer of the particle with a thickness of around 0.1  $\mu\text{m}$ . Due to the constant flow of meteoroids to the lunar surface, it can be assumed that most regolith particles are exposed to solar-wind protons over a sufficiently long time, and the appropriate chemical processes occur in the near-surface layer of each of these particles. Finally, the  $\text{Ag}_2\text{S}$  molecules in the near-surface layer (with a thickness of around 0.1  $\mu\text{m}$ ) of each regolith particle where these molecules were present are replaced by water molecules. Thus, it can be supposed that the water molecules formed by the mechanism described in this study are present only in the near-surface (with a thickness of around 0.1  $\mu\text{m}$ ) layer of the regolith particle. Accordingly, the amount of water in the lunar regolith with respect to the amount of silver sulfide can be estimated as the ratio of the volume of the given near-surface layer of the particle to the volume of a typical regolith particle with a size of several tens of micrometers. In view of the fact that the content of  $\text{Ag}_2\text{S}$  in some areas of the lunar regolith can reach values on the order of 1% (Bogatikov et al., 2001), we find that the fraction of water in the same areas formed by the mechanism described here can exceed  $10^{-6}\%$ .

### Summary

Thus, a mechanism for the reactions of metal sulfides with the use of the energy of solar wind protons has been proposed. It is shown that in this way an oxygen atom from regolith can be launched into the chemical cycles on lunar surface.

As a whole an important component of the formation of iron oxide considered in this work is the presence of the solar wind, the intensity of the interaction of which with the lunar surface is maximum near the equator and minimum in the region of the poles. Accordingly, one should expect that the efficiency of the considered process of iron oxide formation should depend on the lunar latitude. According to (Li et al., 2020) the regions of the presence of iron oxide according to the data of work for lunar latitudes from  $75^\circ$  to  $90^\circ$ . A pattern may be seen wherein the number of areas of iron oxide increases with the distance from the poles of the Moon.

### References

- Bogatikov, O.A., Gorshkov, A.I., Mokhov, A.V., Ashikhmina, N.A., and Magazina, L.O., The first finding of native molybdenum, silver sulfide, and iron-tin alloy in the lunar regolith // *Geochem. Int.*, —2001, —Vol. 39, №. 6, —P. 604–608.
- Dubinsky A.Yu. and Popel S.I., On a Possible Process for the Formation of Iron Oxide in the Lunar Regolith, *Solar Syst. Res.*, —2021, —Vol. 55, №. 4, —P. 307–312.
- Dubinsky A.Yu. and Popel S.I., Water Formation in the Lunar Regolith, *Cosmic Res.*, —2019, —Vol. 57, №. 2, —P. 79–84.
- Golub', A.P., Dol'nikov, G.G., Zakharov, A.V., et al., Dusty plasma system in the surface layer of the illuminated part of the Moon, *JETP Lett.*, —2012, —Vol. 95, №. 4, —P. 182–187.
- Hapke, B., Space weathering from Mercury to the asteroid belt, *J. Geophys. Res.*, —2001, —Vol. 106, №. E5, —P. 10039–10073.
- Li, S., Lucey, P.G., Fraeman, A.A., Poppe, A.R., Sun, V.Z., Hurley, D.M., and Schultz, P.H., Widespread hematite at high latitudes of the Moon, *Sci. Adv.*, —2020, —Vol. 6, №. 36, art. id. eaba1940.
- Mitrofanov, I.G., Sanin, A.B., Boynton, W.V., et al., Hydrogen mapping of the lunar south pole using the LRO neutron detector experiment LEND, *Science*, —2010, —Vol. 330, —P. 483–486.
- Nekrasov, B.V., *Osnovy obshchei khimii (Fundamentals of General Chemistry)*, Moscow: Khimiya, —1973, —P. 594, 606.
- Popel S.I., Zelenyi L.M., Golub' A.P., Dubinskii A.Yu. Lunar dust and dusty plasmas: Recent developments, advances, and unsolved problems, *Planetary and Space Sci.*, —2018, —Vol. 156, —P. 71–84.
- Starukhina, L., Water detection on atmosphereless celestial bodies: Alternative explanations of the observations, *J. Geophys. Res.*, —2001, —Vol. 106, №. E7, P. 14701–14710
- Volkov, A.I. and Zharskii, I.M., *Bol'shoi khimicheskii spravochnik (Large Chemistry Reference Book)*, Minsk: Sovremennaya Shkola, —2005, —P. 70.

### Shornikov S.I., Yakovlev O. I. Experimental study of evaporation of the Ca–Al–inclusions of chondrite melts.

V. I. Vernadsky Institute of Geochemistry & Analytical Chemistry RAS, Moscow, sergey.shornikov@gmail.com

**Abstract.** The results of mass spectrometric experiments on the evaporation of the main types of Ca–Al–inclusions in chondrites (A and B) in the temperature range of 1300–2600 K are presented. The temperature regularities of the appearance of the dominant oxide vapor species in the gas phase over of inclusions show their approximate similarity. The peculiarity of the evaporation of Ca–Al–inclusions in chondrites of types A and B is the preservation of silicon component in the residue melt up to high temperatures exceeding 2500 K. The experimental results show that the high-temperature evaporation of Ca–Al–inclusions in comparison with the carbonaceous chondrite substance, occurs in an oxygen-rich atmosphere. In this regard, it can be assumed that the condensation of the first mineral products in CAIs also occurs in an oxygen environment.

**Keywords:** *evaporation, condensation, Ca–Al–inclusions in chondrites of types A and B*

Ca–Al–Inclusions of chondrites (CAIs) are unique objects of meteoritics. They represent the most primitive matter of the Solar System with an age of 4.567 billion years. CAIs were formed by

condensation of a gas of solar composition. According to modern concepts, evaporation processes also played a significant role in the formation of the compositions of inclusions.

There are two main types of inclusions – types A and B, which differ in mineralogical and chemical compositions. Type A mainly consists of melilite  $\text{Ca}_2(\text{Mg,Al})[(\text{Al,Si})_2\text{O}_7]$  ( $\geq 80$  vol. %) and spinel (5–15 vol. %). Type B consists of melilite (60–70 vol. %), fassaite  $\text{Ca}(\text{Mg,Al,Ti}^{+3},\text{Ti}^{+4})[(\text{Al,Si})_2\text{O}_6]$  (10–25 vol. %), spinels (~10 vol. %). Type A is richer than type B in calcium and aluminum oxides and noticeably poorer on MgO and  $\text{SiO}_2$ . Experimental data on the evaporation of CAIs types A and B are compared with those for Murchison chondrite (CM2) obtained by Yakovlev et al. (1987). Typical compositions of inclusions of types A and B (Grossman et al., 2000), as well as Murchison chondrite (Diakonova et al., 1979) are given in Table 1.

**Table 1.** Initial compositions of CAIs types A and B and Murchison chondrite (wt. %)

Oxide	A	B	M
CaO	36.2	27.6	4.4
MgO	5.0	11.4	47.2
$\text{Al}_2\text{O}_3$	38.3	32.3	2.5
$\text{SiO}_2$	20.5	28.7	45.9

Experimental data on the evaporation of CAIs melts of types A and B at 1300–2600 K were obtained by the Knudsen effusion mass spectrometric method. The studied compositions were natural inclusions of the Efremovka meteorite (CV3) and contained some oxides of potassium, sodium, sulfur, iron, titanium, chromium and nickel. The temperature regimes of the experiments were quite close, as can be seen from Fig. 1.

Samples weighing 10–15 mg were placed in a tungsten effusion cylindrical cell heated by electron bombardment from tungsten cathodes. The ionization of the molecular beam from the effusion cell was carried out by an electron shock at an energy of ionizing electrons equal to 28 eV. The following ions were detected in the vapor mass spectra above the studied melts:  $\text{Ca}^+$ ,  $\text{Mg}^+$ ,  $\text{Al}^+$ ,  $\text{AlO}^+$ ,  $\text{Al}_2\text{O}^+$ ,  $\text{SiO}^+$ ,  $\text{SiO}_2^+$ ,  $\text{O}_2^+$ , as well as  $\text{K}^+$ ,  $\text{Na}^+$ ,  $\text{SO}_2^+$ ,  $\text{Fe}^+$ ,  $\text{Ni}^+$ ,  $\text{Cr}^+$ ,  $\text{TiO}^+$ ,  $\text{TiO}_2^+$ . The  $\text{WO}_2^+$  and  $\text{WO}_3^+$  observed molecular ions corresponded to gaseous tungsten oxide formed due to the interaction of oxygen contained in the gas phase with the material of the tungsten effusion cell.

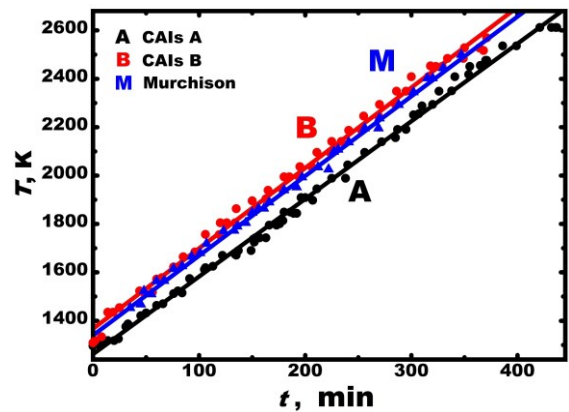


**Fig. 1.** Temperature regimes of experiments on evaporation of CAIs melts of types A and B and Murchison chondrite.

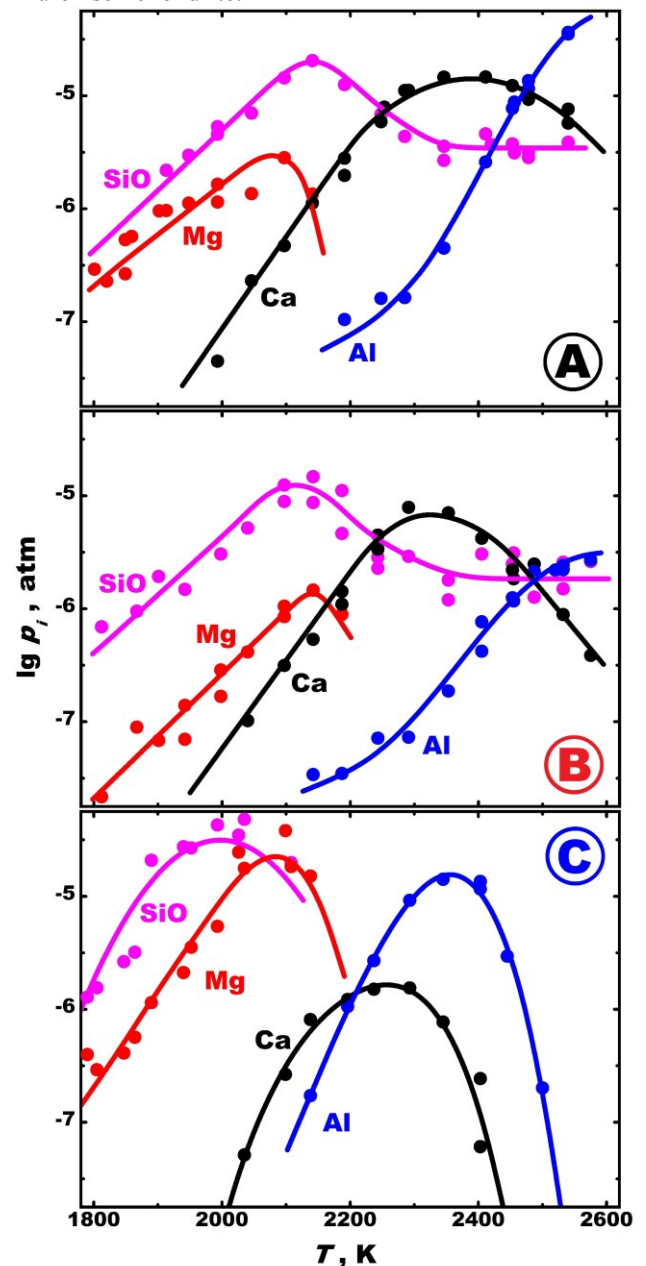


**Fig. 2.** The partial pressures of vapor species (Ca, Mg, Al and SiO) over CAIs melts of types A and B (A, B), as well as Murchison chondrite (C) during evaporation at 1800–2600 K.

A comparison of temperature dependencies of partial pressures of vapor species over CAIs melts of types A and B shows their approximate similarity (Fig. 2, A and B). It is possible to notice the predominance of vapor species corresponding to a higher content of calcium and aluminum oxides in the melt in the case of CAIs type A (Fig. 2A), and for the case of CAIs type B – the predominance of vapor species corresponding to a higher content of magnesium and silicon oxides in the melt (Fig. 2B). An important feature of the evaporation of CAIs types A and B is the preservation of silicon component in the residue melt up to high temperatures exceeding 2500 K.

A comparison of the temperature dependencies of partial pressures of vapor species over CAIs melts of types A and B with that for the case of Murchison chondrite (Fig. 2C) shows that the latter has a slightly higher volatility at 1800–2100 K, due to the high content of magnesium and silicon oxides in the melt (compared with CAIs types A and B) and almost completely evaporates at 2200–2300 K.

As follows from Fig. 3, the evaporation of CAIs melts of types A and B occurs with the release of a significant amount of oxygen from the melt compared to that for Murchison chondrite (Fig. 3). The melt behavior during high-temperature evaporation indicates that the process takes place in an oxygen-enriched atmosphere. It can then be assumed that the condensation of the first mineral products of CAIs also occurs in an oxygen environment.

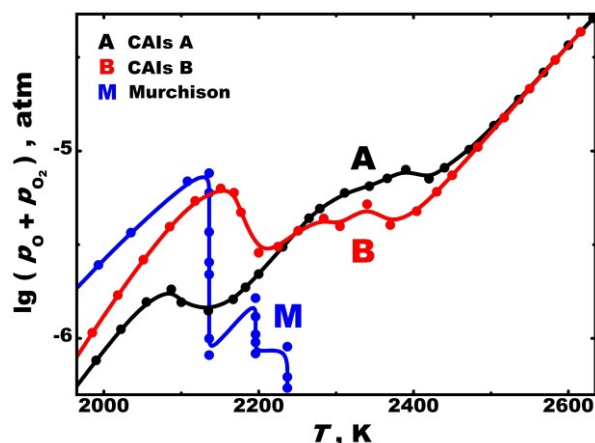


Fig. 3. The temperature dependencies of oxygen pressure over CAIs melts of types A and B and Murchison chondrite during evaporation.

#### References

- Dyakonova M. I., Kharitonova V. Y., Yavnel A. A. (1979) Chemical composition of meteorites. Moscow: Nauka, pp. 1–68 [in Russian].  
 Yakovlev O. I., Markova O. M., Belov A. N., Semenov G. A. (1987) On the formation of a metallic form of iron

during heating of chondrites. *Meteoritics*, no. 46, pp. 104–118 [in Russian].

- Grossman L., Ebel D. S., Simon S. B., Davis A. M., Richter F. M., Parsad N. M. (2000) Major element chemical and isotopic compositions of refractory inclusions in C3 chondrites: the separate roles of condensation and evaporation. *Geochim. Cosmochim. Acta*, vol. 64, no. 16, pp. 2879–2894.

#### Tselmovich V.A.<sup>1</sup>, Maxe L P.<sup>2</sup> Recognition of cosmic and atmospheric dust particles. UDC 628.511

<sup>1</sup>Borok Geophysical Observatory, the Branch of Schmidt Institute of Physics of the Earth, Russian Academy of Sciences, Borok, Yaroslavl oblast, 152742 Russia  
 tselm@mail.ru,

<sup>2</sup>Belarusian State University of Food and Chemical Technologies (BSUT), Belarus, Mogilev, ave. Schmidt, 3,  
 larissa\_maxe@rambler.ru,

**Abstract.** The authors compared magnetic particles contained in the sediment of urban atmospheric dust with particles related to cosmic dust, which were preserved in ancient sedimentary rock. Mt-microspheres, as well as magnetic particles in the form of twists and shavings, are present both in sedimentary rocks and in settled urban atmospheric dust. Particles extracted from urban dust cannot be attributed by their origin to cosmic particles without special research. Magnetic particles in the form of twists and shavings contained in ancient sedimentary rocks cannot have man-made origin, their terrigenous origin is unlikely, but their formation is possible during the destruction of meteoroids. Magnetic particles in the form of twists and shavings with traces of deformation (the action of friction, shear, stretching forces) are attributed to particles formed in the body of a meteoroid as a result of internal processes leading to the destruction and dispersion of most of its initial substance in the Earth's atmosphere.

**Keywords:** Mt-microspheres, morphology, meteoroid, cosmic, atmospheric dust.

**Introduction.** The importance and meaning of the influence of cosmic dust particles (CD) on global processes in the atmosphere has been increasing dramatically recently for many reasons, including climatic ones. In this regard, the number of analytical and practical tasks for studying the processes of formation, movement, deposition of CD on the Earth's surface is increasing. Space flows of matter, comets, meteoroids are considered to be the sources of receipt of CD (Bochkarev N.G. et al., 2014).

The similarity of the morphology and composition of the cosmic and technogenic components of urban atmospheric dust (UAD) often leads to the fact that the predominant technogenic component is attributed to the cosmic. At the same time, there are a number of references to the works of authors who studied the CD and provided evidence that the detected dust is cosmic. The emerging information noise disorients both researchers and the

population, and is a powerful pseudoscientific component that often present in both the scientific and popular press. Previously, we studied the composition and morphology of CD particles in sedimentary rock (trepel) older than 30 million years, as well as technogenic dust particles for analytical comparison and subsequent application in solving a new problem (Tselmovich, Maxe, 2022).

The task we have set does not concern the quantitative calculation of CD particles in the UAD that has settled on the surface – the roof of the building, selected as a collection plate for sediment containing CD. The aim of the work is to identify differences between magnetic particles of CD in the UAD sediment, including technogenic, and CD particles that have been preserved in the ancient sedimentary rock – trepel of the Stalnoye deposit, a priori containing no technogenic particles.

**Materials and methods.** Samples of atmospheric dust (in Mogilev) from plastic storage devices (prefabricated trays) were selected as a comparison material. The magnetic component was separated by a method almost analogous to the separation of CD from sedimentary rocks. We attributed the elemental composition, particle size and shape, morphology, known or suspected pathway or process of their formation to the potentially possible differences between magnetic CD particles in the UAD sediment and magnetic CD in sedimentary rock. From the database of studies carried out earlier and in this work, we selected information about the chemical composition, particle images obtained on a scanning electron microscope (SEM) Tescan Vega II (GO Borok, IPE RAS), a Nikon polarization microscope (BGUT, Mogilev). The images obtained using Nikon, the non-magnetic part of urban dust and magnetic extraction from that are shown in Fig. 1.



**Fig. 1.** Images (Nikon): **a** – non-magnetic part of the UAD sample; **b, c** – magnetic fraction separated from the sample UAD (with fine mineral admixture).

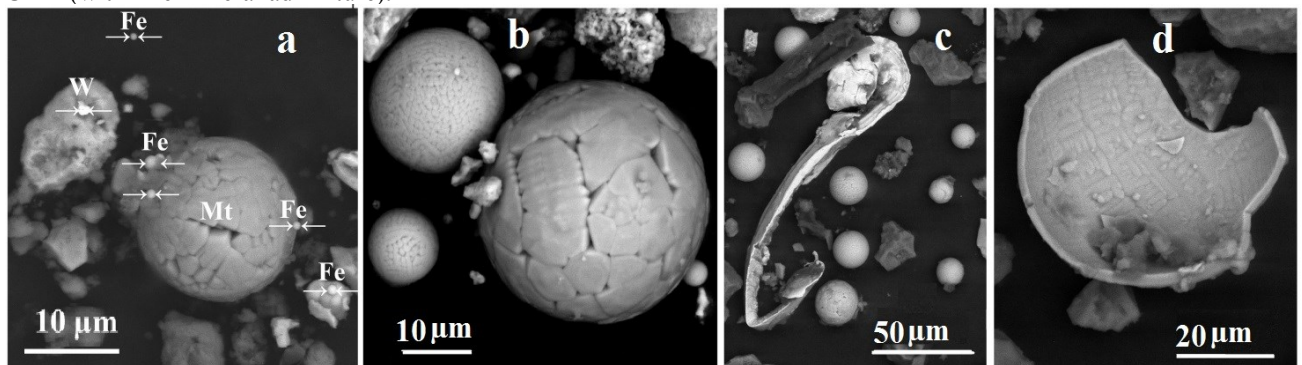


**Fig. 2.** SEM Images: **a, b** – Mt-microspheres extracted from sedimentary rocks (opoka, trepel), **c, d** – Mt-microspheres separated from the UAD sample (curved metal particle – in the center of "c").

For the purpose of comparative analysis, images of magnetic particles separated from sedimentary rocks, containing CD, as well as images of UAD particles, were distributed according to the "method of their production" – the mechanism of formation during the destruction of the source material. Magnetic particles spherical in shape were attributed to particles obtained in high-temperature processes,

in the case of a meteoroid, this is ablation occurring in its surface layers when moving in the atmosphere, in the case of man-made processes, artificial ablation of materials (during welding, in an electric arc, plasma cutting, plasma spraying, etc.). In Fig. 2 the Images of Mt-microspheres obtained using SEM are presented.

Magnetic particles in the form of chips are

attributed by us to particles formed in the processes of physical and mechanical transformations leading to the destruction of part of the source material. Particles in the form of chips are formed in many technogenic processes. Metal processing (cutting, turning, grinding), friction in parts, nodes, contacts are accompanied by the formation of particles: chipping, drain chips, element chips, breakage chips (Zubarev, Priemyshev, 2010).

Among the Mt-microspheres contained in sedimentary rocks, we previously identified magnetite dendritic microspheres with thick walls, thin-walled – ablative, and the presence of very small iron microspheres formed outside the oxidizing medium was also noted. Mt- and metal microspheres are formed during the ablation of meteoroid matter, they settle on the Earth's surface often after a long stay in atmospheric flows. We also found Mt-microspheres in the UAD, similar in composition and morphology to microspheres contained in sedimentary rocks (peat, trepel, bottom sediments of swamps), but their attribution to CD particles is ambiguous and is accompanied by questions.

Microparticles in the form of chips were also found in the sample and magnetic extracts from the

UAD, but their presence is understandable due to the presence of urban technogenic sources. Comparison with the particles-shavings extracted from the UAD raises the question of the "origin" of particles similar to them in shape and morphology – curls, shavings, twists, scales, found in a variety of sedimentary rocks and media (trepel, peat, bottom sediments of swamps). The absence of technogenic sources of micro chips formation in an uncontaminated ancient sedimentary rock is a priori and does not require proof. Currently, representations based on research and computer, mathematical modeling of the processes of movement and destruction of meteoroids in the Earth's atmosphere have a convincing evidence base for the possibility of formation and deformation of particles in the body of a meteoroid moving in the Earth's atmosphere at supersonic speed, due to the fact that internal friction and stress forces arise in its inner part, leading to its destruction and separation into many fragments and small particles which are prolong moving and fall through the atmosphere (Tirskyi, 2021; Syzranova, Andrushchenko, 2022).

Fig. 3 shows the SEM images of magnetic particles having the form of chips, curls, twists.

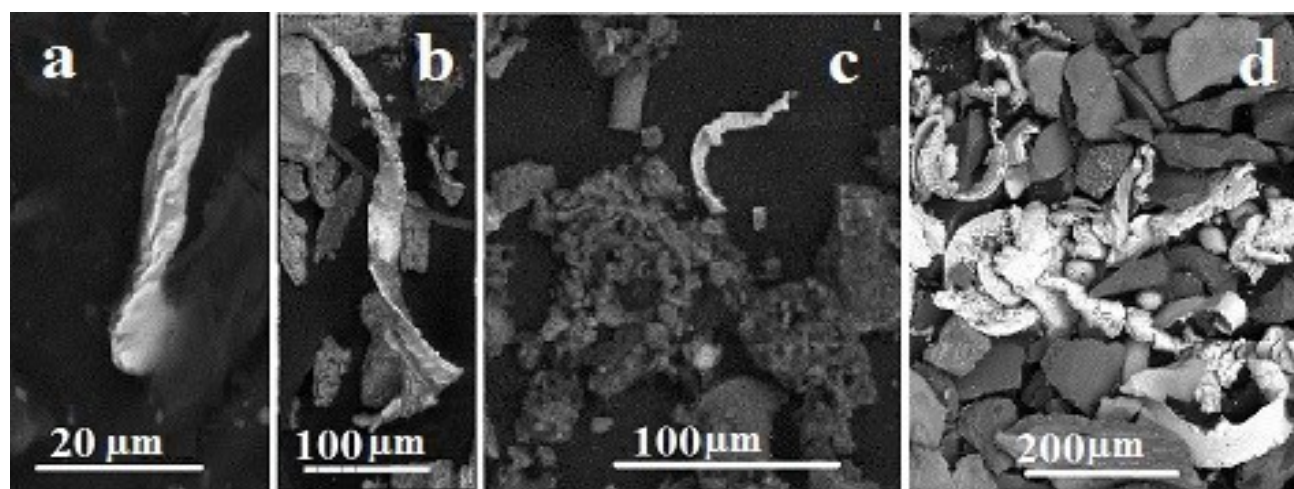


**Fig. 3.** SEM Images: **a** – an iron particle extracted from trepel; **b** – an iron particle extracted from peat; **c** – an iron particle in UAD sample; **d** – chip particles formed during the processing of steel (ice skating blades) with a grinding wheel (made of white corundum with diamond dust).

**Results and discussion.** Almost all iron particles extracted from ancient sedimentary rocks have characteristic features – traces or signs of the impact of tensile forces, shear deformation or shock destruction on them. Scientists explain the nature of deformation and subsequent destruction of the meteoroid by the presence of internal friction forces as tangential stresses proportional to pressure, confirming the actual material with appropriate mathematical calculations (Shuvalov, Trubetskaya, 2010).

Figure 4 shows the SEM images of iron particles extracted by a magnet from an ancient marine sedimentary rock – trepel, which was formed more than 30 million years ago. The iron particles in the SEM images (Fig. 4) have traces of viscous destruction. In the process of plastic flow of metal, pits of viscous destruction appear in its structure – microscopic depressions on the surface that has been strongly affected. Elongated shear pits are formed by destruction forces and are elongated in one direction. Separating dividing lintels are formed as a result of

the stressed state of the particles when the impact strength is manifested. Theoretically, two elementary mechanisms of destruction are considered – the separation of the body into two parts. In one of the variants, a mechanism is implemented when there is a sequential break of atomic bonds along the crystallographic plane, chipping and sliding along a certain plane is carried out as a plastic shear (Fig. 4, a). Chipping is possible without the participation of plastic deformation – this is a fragile destruction. In

the second variant of the mechanism new surfaces arise as a result of slippage (sliding), with this mechanism, the separation into parts is preceded by a large plastic shift and a large amount of plastic deformation work, and a cut result is observed as a viscous destruction, in this case many initial elements merging in micropores. A characteristic sign of viscous plastic destruction is elongated pits as parts of fused pores (Fig. 4, c).

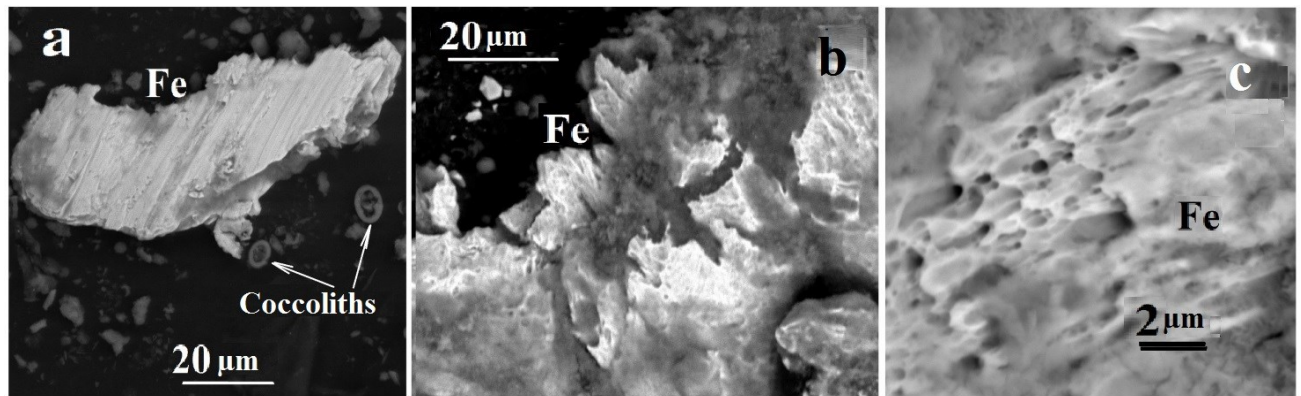


**Fig. 4.** SEM Images: **a** – iron particle extracted from trepel (containing microfossils – coccoliths) with a clear cut trace on the surface; **b** – iron particle whose edge has undergone plastic deformation; **c** – pits of viscous plastic destruction of metal.

**Conclusions.** Mt-microspheres, varying in size, but similar in composition, shape and morphology, as well as magnetic particles in the form of micro chips and twists are contained both in sedimentary rock and in the UAD. However, without additional research, Mt-microspheres and magnetic particles in the form of chips contained in the UAD cannot be attributed by origin to CD particles. At the same time, magnetic particles in the form of twists and shavings contained in ancient sedimentary rock cannot have a man-made origin, their terrigenous origin is unlikely, but their formation in the process of destruction of meteoroids is possible, which is confirmed by computer mathematical modeling and explains the actual material: the destruction of most of the substance of meteoroids to particles related in size to the cosmic dust particles and atmospheric dust particles at the same time.

The work was carried out within the framework of the state task of the IPE RAS (№ FMWU-2022-0026).

#### References

1. Bochkarev N.G. Problems of studying cosmic dust on Earth (To the research program) / Edited by N. G. Bochkarev: comp. L. M. Gindilis, M. I. Kapralov. – Dubna: JINR, 2014. – 87 P.
2. Zubarev Yu.M., Priemyshev A.V. Theory and practice of improving the efficiency of grinding materials. Publisher: Lan, 2010. – 303 P.
3. Syzranova N.G., Andrushchenko V.A. Numerical modeling of physical processes leading to the destruction of meteoroids in the Earth's atmosphere. Computer research and modeling. 2022. Vol. 14, № 4, P. 835 – 851.
4. Tirskiy G.A. Aerothermoballistics of crushing meteoroids in the Earth's atmosphere. Applied Mathematics and Mechanics. 2021. T. 85, № 5, P. 635 – 663.
5. Tselmovich V.A., Maxe L.P. Microstructure and composition of magnetic microspheres of anthropogenic and cosmogenic origin. Proceedings of the All-Russian Annual Seminar on Experimental Mineralogy, Petrology and Geochemistry. (RASEMPG-2022), GEOCH RAS, Moscow, April 19 – 20, 2022, P. 340 – 345.
6. Shuvalov V.V., Trubetskaya I.A. The effect of internal friction on the deformation of a destroyed meteoroid. Astronomical Bulletin, 2010. vol. 44, № 2, P. 117 – 122.

**Tselmovich V.A.<sup>1</sup>, Shelmin V.G.<sup>2</sup> Meteorite, blast, or natural fire? UDC 523.6; 669.1; 614.841**

<sup>1</sup> Borok Geophysical Observatory, the Branch of Schmidt Institute of Physics of the Earth, Russian Academy of Sciences, Borok, Yaroslavl oblast, 152742 Russia

**Abstract.** The Chulymsky bolide arrived and broke out at an altitude of about 100 km on February 26, 1984 in the evening of February 26, 1984 near the Chulym River (a tributary of the Ob) on the border of the Krasnoyarsk Territory and the Tomsk region. Samples similar to meteorite fragments were collected. However, the study of their composition with the help of a microprobe did not allow us to assert that the stones found are of meteoritic origin. Rather, it could be assumed that they were formed as a result of a process resembling a domain. However, there was no modern metallurgical production near the site of the find. The next version of the origin of the finds is a powerful natural fire. The findings are unusual, and the authors tried to explain the nature of the findings and substantiate various hypotheses.

*Keywords:* Chulym space body, impact event, cosmogenic substance, ferrite-perlite microstructure, stages of the domain process.

## Introduction

Meteorites are valuable for science, as they tell about the composition and structure of extraterrestrial bodies. Those who watched the fall of the car are often shocked by what they saw, and have been looking for a fallen stone for decades. The Chulym space body (CSB) entered the Earth's atmosphere on the evening of February 26, 1984. It broke out at an altitude of about 100 km near the Chulym River (a tributary of the Ob River) on the border of the Krasnoyarsk Territory and the Tomsk region. The car was observed for about 10 seconds as a flight of an extremely bright sparkling object, which was accompanied by a shock sound wave and a micro-earthquake recorded by regional stations of the Unified Network of Seismic Observations. According to experts, it had a capacity of over 11 kilotons in TNT equivalent.

The flight of the CSB was observed from east to west. A crater was found along the flight path, located 6 km to the northeast of the found debris scattering and a little to the north. Eyewitnesses (there is a questionnaire) and personally Shelmin V.G. confirm that the car sparkled at high altitude. It is noted that fragments were separated from the car until the final stage of the flight. The funnel, in which a scattering of gray-metal fragments were found, is located in the floodplain of the Ob river (300 meters to the shore of the channel), the alley of the lake and the swamp 5 km. The funnel is an oval of 6X8 meters. It is oriented from east to west, its depth is about 3 meters. There is a dump around the perimeter with a height of about a meter in relation to the surrounding surface. Groundwater in the center of the funnel in July 2022 was recorded at a depth of 1 meter.

## Materials and methods. Investigation of the impact area of a meteor explosion

In the summer of 1984, the expedition of the Institute of Geology and Geography of the Siberian Branch of the USSR Academy of Sciences, which was searching for the debris of an exploded cosmic body, did not find any traces that could be unambiguously associated with the hypothetical substance of the bolide. Further official expeditions were not carried out, but the search work continued in independent groups. In the last 10 years, using modern technical means, it has been possible to find more than 100 fragments that are not typical for the territory of their discovery. The fragments were found in a meadow with a fertile layer thickness of 10-20 cm, below which there is brown clay (Fig.1a, b).



a) b)

**Fig. 1.** a) A general view of a meadow with stone fragments; b) a stone fragment.

## Results of microprobe analysis of stone fragments

The methods of optical and electron microscopy were used to analyze the stone fragments found in the area of the alleged impact of CSB. The micromineralogical analysis was carried out using a scanning electron microscope "Tescan Vega II" with a prefix for energy dispersion analysis.

In sample 5, both iron oxides and metallic iron were found, that is, different stages of the process. Iron oxides were found in soil samples (Fig.2a, b).

Preparations from magnetic and non-magnetic fractions of soil particles from a "shock" funnel were studied. The magnetic part contained mainly iron oxides (Fig.2a, b), the non-magnetic part contained quartz, aluminosilicates, calcites, ilmenite, etc.

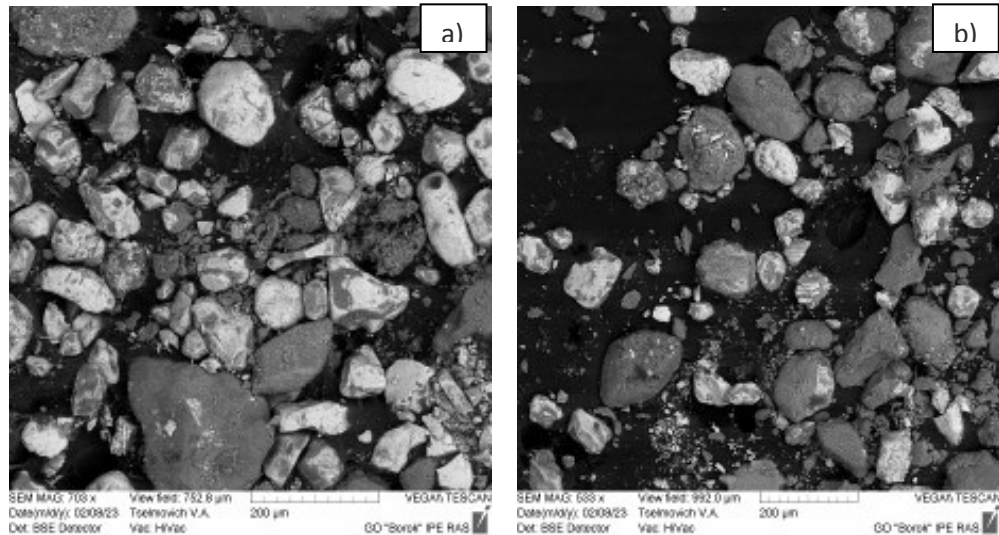


**Fig.2.** Magnetic fraction of soil particles from the "shock" funnel (a) and from the soil in the meadow (b). Light particles - iron oxides.

Iron droplets with a ferrite-perlite lamellar structure were found in the anschlyphs of the six fragments studied. No information has been found regarding analogues of such structures in meteorites. Alumomagnetic silicates and calcites surrounding iron droplets have a different chemical composition,

which is close to the composition of sandstone minerals consisting of quartzite with an admixture of clay substances, alumomagnetic silicates and calcites. Carbon was found in all samples in the form of films and separate carbonaceous secretions. In general, the samples resemble blast furnace slag.

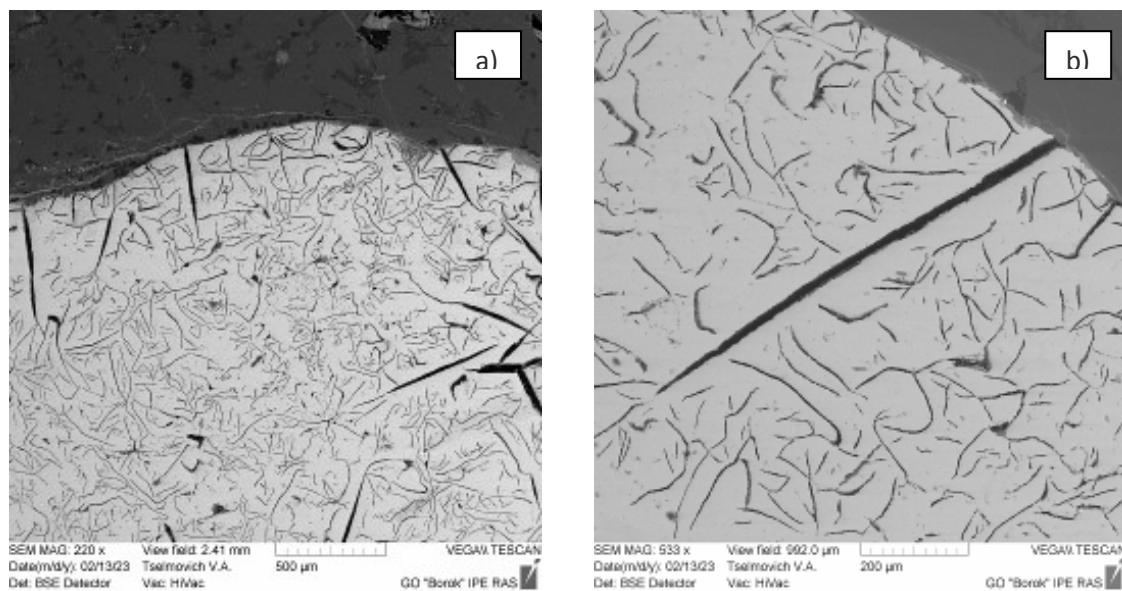


**Fig.3.** Sample 1. a) grav ferrite-pearlite cast iron, the structure of which consists of ferrite + pearlite and plate inclusions of graphite. b) – a grain fragment.

**Discussion.** The studied samples had no pronounced signs inherent in a cosmogenic meteoritic substance: they did not have a melting crust, they were porous, very brittle, and did not

contain nickel.

Similar samples were repeatedly received by the author (V.A. Tselmovich) from various sources for the purpose of diagnosing them as meteorites, and

were rejected due to the absence of signs of cosmogenicity and the presence of signs of a domain process. Dense samples contained gray ferrite-pearlitic cast iron (Fig.3a, b), the structure of which

consists of ferrite + perlite and graphite inclusions. In this cast iron, the amount of bound carbon is less than 0.8%.

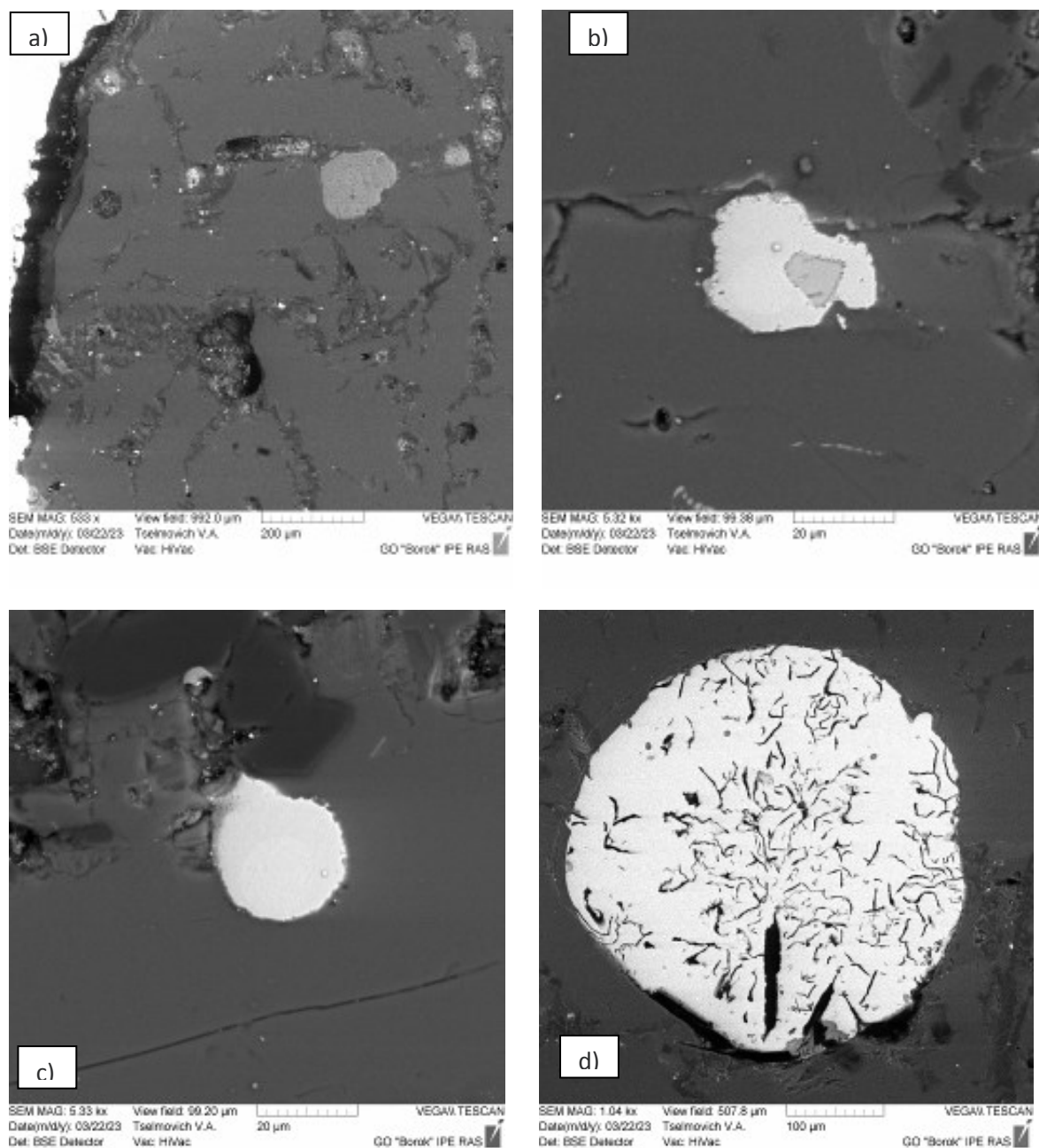


**Fig.4.** a) particles of iron oxides in the marginal zone of the fragment; b) partially reduced iron with iron sulfide residues; c) almost spherical grains of pure iron; d) a drop of gray ferrite-pearlite cast iron with lamellar carbon emissions.

The stages of the iron reduction process can be observed both from sample to sample and in one sample (model 5). Sample 5 contains the initial grains of iron oxides (Fig. 4a), partially reduced iron with iron sulfide residues (Fig. 4b), almost spherical grains of pure iron (Fig. 4b) and gray ferrite-pearlite cast iron (Fig. 4g). Probably, this fragment was

located in the zone of a large temperature gradient, thanks to which all the main stages of the iron recovery and carburization process were visible. Figure 5 shows pure iron particles in the marginal zone of sample 1. In this zone, iron was recovered from iron oxides, but the temperature was insufficient to give the particles a spherical shape.

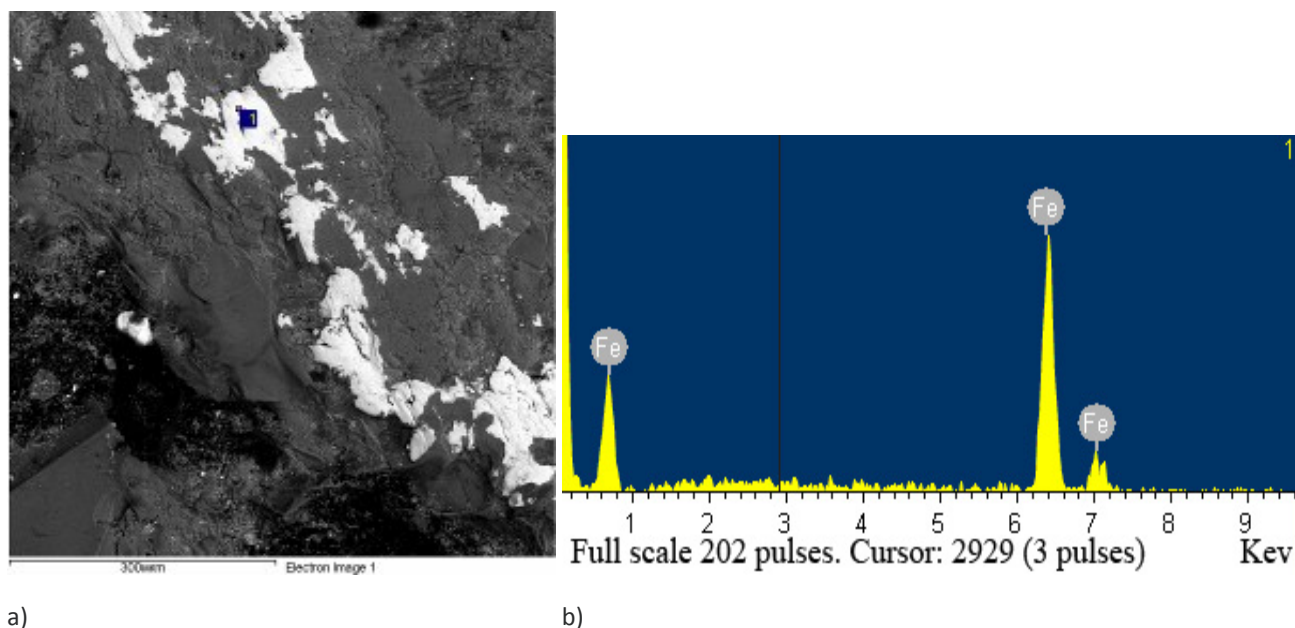


**Fig.5.** a) pure Fe particles in the boundary zone of Model 1; b) a typical spectrum, i.e. 1 in Fig.5 a).

### Conclusions

Usually, researchers in search of traces of impact events focused on the search for massive objects. However, when studying the CSB, the massive objects found in the form of hundreds of fragments are not cosmogenic in terms of the sum of the signs. Our hypothesis of the origin of the funnel is not "shock", but natural, in which a blast furnace-type process was realized, with a powerful natural fire. Then there was an explosion. During the explosion, the stones from the blast furnace were scattered. The authors hypothesized the identification of the found massive fragments as traces of a powerful natural fire, or as slags of ancient metallurgical production [1].

At the same time, the authors do not exclude the comet nature of CSB, which will require searching not for massive fragments of CSB, but for microscopic traces, as was done in [2] by identifying Ni film microstructures.

---

*The work was carried out within the framework of the state task of the IPE RAS (No. FMWU-2022-0026)*

### References

1. Vodiasov E.V. Medieval cheese-making horns of the Shaitan archaeological microdistrict // Vestn. Tomsk State University. 2012. No. 359. pp. 79-83.
2. Tselmovich V.A. Microscopic traces of comets falling to Earth. 4th All-Russian Conference on Astrobiology "Geological, biological and biogeochemical processes in solving astrobiological problems". Abstracts of reports Pushchino, Russia February 27 – March 02, 2023. pp.63-65

### Ustinova G.K. Perspectives of cosmogenic radionuclide research in the fresh fallen chondrites. *UDC 523.165*

V.I.Vernadsky Institute of Geochemistry and Analytical Chemistry (GEOKHI) of RAS, Russian Federation, Moscow [ustinova.gk@mail.ru](mailto:ustinova.gk@mail.ru); [ustinova@dubna.net.ru](mailto:ustinova@dubna.net.ru)

**Abstract.** The elaborated program of cosmogenic radionuclide research in the fresh-fallen chondrites for study of the temporal and spatial variations of the galactic and solar cosmic rays in the Solar system for the long-time scale and at the different heliocentric distances is presented. Previously, the problem was described in detail by Lavrukhhina and Ustinova (1990), and then it was successively supplemented and specified in the numerous later works. In principle, the main role in these researches is played by the proposed and elaborated analytical method of the development of the nuclear cascade in cosmic bodies of different sizes and compositions. The importance of the stratospheric balloon measurements of the GCR intensities for  $E > 100$  MeV is pointed out – as well as the exactness of the low-level measurements of radionuclide contents. The worth of the program of monitoring and photographing of the meteorite falls is stressed.

**Keywords:** chondrites; cosmogenic radionuclides; cosmic rays; Solar system.

The cosmogenic radionuclides with the half-lives from several days (e.g.,  $^{32}\text{P}$  ( $T_{1/2} = 14.3$  days)) up to ~ one billion years (e.g.,  $^{40}\text{K}$  ( $T_{1/2} = 1.48 \cdot 10^9$  years)) could be measured in meteoritic and lunar samples. This provides us with the unique information on evolutionary peculiarities of the extraterrestrial matter in broad intervals of its cosmic age and at

different distances from the Sun. The cosmogenic radionuclides are produced by the galactic and solar cosmic rays (GCR and SCR, successively) in nuclear reactions with the matter of cosmic bodies. The nuclear reaction efficiency is directly proportional to the intensity of the radiation, which allows one to consider the radionuclides as natural detectors of cosmic rays. Meteorites have the orbits of different size and inclination; they fall during the various years of the solar activity. All this presents them as the universal probes of cosmic rays in the three-dimensional heliosphere. However, meteorites have the different chemical compositions as well as the different sizes, which requires the knowledge of the regularities of the GCR and SCR passage through the matter of different composition. Just the cosmogenic radionuclide research was the trigger to the development of the experimental and theoretical methods of measurement of the cross sections and the production rates of radionuclides in thin and thick targets at the accelerators, which enriched so greatly the existing bank of this invaluable information. (Kohman and Bender, 1967; Arnold. Honda, Lal, 1961; Reedy and Arnold, 1972; Lavrukina, 1972).

Simultaneously, theoretical and semi-empirical methods of modeling cascade processes in the frames of the cascade-evaporation model of cosmic radiation passage in cosmic bodies of different sizes and compositions (Arnold. Honda, Lal, 1961; Lal D. 1972; Reedy and Arnold, 1972; etc.), including also the Monte Carlo statistical method (Armstrong. 1969; etc.), started to be developed. All these methods are presented in the book (Lavrukina and Ustinova, 1990), where their advantages as well as weaknesses and complexities for the analysis of measured contents of cosmogenic radionuclides are considered in detail. Just at that early stage of the investigation, the patterns caused by the solar modulation of the GCRs were revealed (Dorman, 1963, etc.). Since the GCR intensity near the Earth is anti-correlated with the solar activity, the contents of the cosmogenic radionuclides with the half-lives of < 5 years (e.g.,  $^{54}\text{Mn}$  ( $T_{1/2} = 300$  days.);  $^{22}\text{Na}$  ( $T_{1/2} = 2.62$

years.);...) turned out to be anti-correlated with the solar activity too, being dependent on the phase of the GCR solar modulation at the moment of the meteorite fall (Evans et al., 1982; Bhandari, et al., 1994; etc.). Certainly, this fact just complicated the possibilities of the analysis of the cosmogenic radionuclide contents in cosmic bodies by the existing methods, because all these methods are constrained to use only some average parameters of both the matter and radiation – whereas, e.g., the every fallen meteorite deserves the specific analysis of its cosmogenic radionuclide content, depending on its composition, size and degree of ablation, on the cosmic ray intensity at the moment of fall and on the extension of its orbit.

Just such problems were raised by us in the proposed and elaborated analytical method for the quantitative description of the depth distribution of cosmic ray intensity and cosmogenic radionuclides in any point of isotropically irradiated cosmic bodies of any size and composition (Lavrukina and Ustinova, 1967). The elaboration of this method, analytical expressions and all the required parameters are presented in detail in (Lavrukina and Ustinova, 1990; Ustinova and Lavrukina, 1990).

The SCR impact areas are the near-surface layers ( up to ~ 10 cm ) of cosmic bodies, which, in the case of meteorites are commonly lost during the ablation (Bhandari et al., 1980). However, it is possible to measure and analyze the radionuclides, produced by the low-energy solar protons, in a number of meteorites with low ablation (Lavrukina and Ustinova, 1971; Ustinova, 2018; 2021). In particular, the dependence of the solar proton effects on the solar activity and on the cross sections of the radionuclide production, as well as on the chemical composition of chondrites, on their preatmospheric sizes, on the extension of their orbits and on the screening of the investigated samples, are investigated by the analytical method in the case of the Stubenberg (LL6), Jesenice (L6), and Bruderheim (L6) chondrites. (Ustinova, 2018). The results are in the Table.

**Table.** The contribution of the solar protons ( $E > 20$  MeV) to the production of the measured radionuclide contents (in dpm/kg) in the Bruderheim, Jesenice and Stubenberg chondrites, which fell, successively, on March 4, 1960 (i.e. at the Maximum phase of the 19 solar cycle), on April 4, 2009 (at the rise of the 24 cycle ) and on March 3, 2016 ( at the decline of the 24 cycle).

	$^{48}\text{V}$	$^{51}\text{Cr}$	$^{46}\text{Sc}$	$^{54}\text{Mn}$	$^{22}\text{Na}$	$^{55}\text{Fe}$	$^{26}\text{Al}$
Buderheim	6.1	122.0	1.5	18.1	15.2	138.5	0.8
Jesenice	0	0	0	0	0.32	2.92	2.1
Stubenberg	0.09	1.85	0.02	5.4	44.4	404.8	2.8

The presented results testify to the complex interactions of various factors for different radionuclides in different chondrites. The exact account of the fraction of the radionuclides produced

by solar protons is required for the investigation of subtle effects of variation of the radiation environment in the Solar system when forecasting the safety of the man-carried space missions.

The stony meteorites, in particular, the ordinary chondrites, are the most abundant and frequently falling meteorites, which provides the most complete accessible information on the temporal and spatial variations of the radionuclide production rates in the internal heliosphere. Meantime, on the other hand, the chondrites are the most complex bodies from the viewpoint of interpretation of the measured radionuclide contents, because the rates of radionuclide production on all the main target

elements of their chemical composition should be taken into account.

A cascade of the secondary particles of different stages of generation develops under isotropic irradiation of chondrites in space, so that the production rate of  $i$ -radionuclide in the chondrite of radius  $R$ , at the distance  $r$  from its center, could be approximated in the following analytical form (Ustinova and Lavrukhina, 1990; Ustinova, 2016; Ustinova and Alexeev, 2020):

$$H_i(R, r) \approx \left[ I_p(R, r) \sum_{j=1}^n \frac{N}{A_j} m_j \bar{\sigma}_{ij}^p + \sum_s I_s(R, r) \sum_{j=1}^n \frac{N}{A_j} m_j \bar{\sigma}_{ij}^s + \sum_t I_t(R, r) \sum_{j=1}^n \frac{N}{A_j} m_j \bar{\sigma}_{ij}^t + \dots \right] \quad (1),$$

where  $N$  is the Avogadro number,  $I_{p,s,t}(R, r)$  are the integral fluxes of primary, secondary and tertiary particles,  $\bar{\sigma}_{ij}^{p,s,t}$  are the mean-weighted production cross sections of  $i$ -radionuclide from  $j$ -target of mass number  $A_j$  for primary, secondary and tertiary particles, for instance:

$$\bar{\sigma}_{ij}^p = \int \frac{\sigma_{ij}^p(E) F^p(E)}{F^p(E)} dE, \quad (2)$$

and  $m_j$  is the abundance of  $j$ -target element in a chondrite. Then, the radionuclide production rate  $H_i$  at the heliocentric distance  $\tilde{r}$  is proportional to the integral GCR intensity  $I_{\tilde{r}}(>E)$  at the heliocentric distance  $\tilde{r}$ , and  $H_{\oplus}$  is that near the Earth, which is proportional to the integral GCR intensity  $I_{\oplus}(>E)$  at 1 AU. Introducing a “gradient” of the radionuclide production rate in the heliosphere as

$$G_{\tilde{r}}^H = \frac{H_{\tilde{r}} - H_{\oplus}}{\tilde{r} - 1} \cdot 100\% \quad (3),$$

where  $H_{\tilde{r}}$  is the measured content of a radionuclide in the chondrite, and  $H_{\oplus}$  is its content in the same chondrite, calculated using GCRs at 1 AU (stratospheric data), we obtain for the gradient of the integral GCR intensity

$$G_{\tilde{r}}^{I_{\tilde{r}}(>E)} = \frac{I_{\tilde{r}}(>E) - I_{\oplus}(>E)}{\tilde{r} - 1} \cdot 100\% \quad (4),$$

where  $E \geq 100$  MeV (see above). The direct proportionality of both the gradients to the integral intensity of GCRs ( $E > 100$  MeV) is natural, which allows us to obtain some indirect information on the GCR distribution and variations at different heliocentric distances and during different time periods in the Solar system for the long-time scale over the last  $\sim 1$  Myr. Such a rare possibility is not yet available for direct measurements in the interplanetary space, moreover, in the volumes that constantly falling chondrites can provide.

At the depths of  $\geq 10$  cm from the surface of cosmic bodies, the cosmogenic radionuclides are mainly produced by the GCRs with  $E \geq 100$  MeV and, thus, just in this range the variations of the GCR intensity should be taken into account for the appropriate analysis of their contents. The balloon measurements of the intensity of the primary component of the GCRs with  $E \geq 100$  MeV, being fulfilled since 1957 at the initiative of S.N. Vernov, present the unique continuous and homogeneous set of such data (Stozhkov, et al., 2009). That made it possible, for the first time, to investigate the variations of the gradients of the radionuclide production rates as compared with the variations of the GCR gradients in the internal heliosphere.

Up to nowadays, the production rates of cosmogenic radionuclides in 42 chondrites, having fallen in 1959-2016, are studied (Fig. 1).

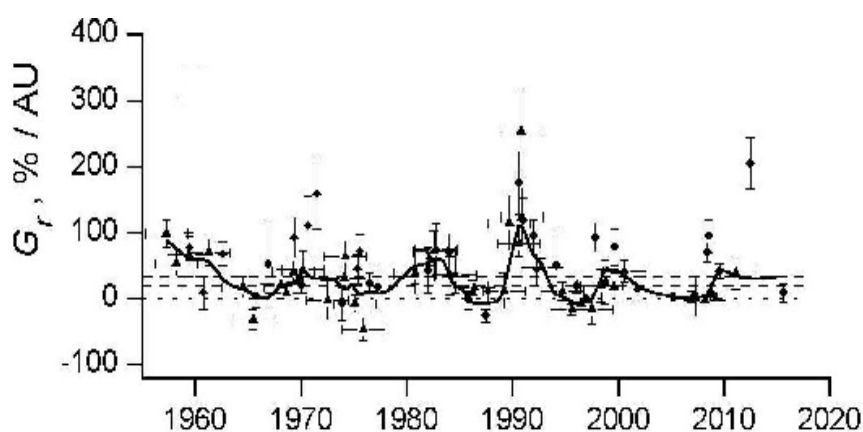


**Fig.1.** Variations of integral gradients of the cosmogenic radionuclide production rates along the orbits of 42 chondrites having fallen in 1959-2016, according to the data on radioactivity of:  $^{54}\text{Mn}$  (circles),  $^{22}\text{Na}$  (triangles) and  $^{26}\text{Al}$  (dashed horizontals at 20-30%/AU) (Ustinova and Alexeev, 2020). The solid curve is a polynomial curve of the experimental data smoothing over 5 points with taking into account the statistical weight of each of the points. The unknown orbits of some chondrites are determined by the phenomenological method (Lavrukhina and Ustinova, 1971; 1990). The GCR ( $E > 100$  MeV) intensity variations near the Earth are from the data of (Stozhkov, et al., 2009).

According to Fig.1, one may see the long set of homogeneous data on the  $^{54}\text{Mn}$  and  $^{22}\text{Na}$  production rates at the heliocentric distances up to  $\sim 5$  AU during  $\sim 6$  solar cycles. The comparison of this set with the existing long sets of the homogeneous data on the solar activity <http://sidc.oma.be/silso/> and on the stratospheric data regarding the intensity of GCR ( $E > 100$  MeV) near the Earth (Stozhkov et al., 2009) shows that, contrary to the anti-correlation of the radionuclide production rates and the GCR intensity with the solar activity, the gradients of the radionuclide production rates correlate with the solar activity, i.e., they develop just during the years of the active Sun.

On the average, the gradients of the cosmogenic radionuclides production rates are always higher than the integral GCR gradients equaling  $\sim 2-4$  %/AU (Potgieter, 2013), conditioned by the entire volume of the solar wind. The fact is that, in the years of the high solar activity, the dynamics and configuration of the magnetic fields in the heliosphere vary (Parker, 1979), and they become already azimuthal at  $\sim 5$  AU. In addition to the regular magneto-hydrodynamical processes, the stochastic ones (including those in the operation of the Sun dynamo) also arise, which hinders the GCR passage to the Sun. It is seen that just the variation of the magneto-hydrodynamical conditions of the environment during the years of the active Sun is the reason for the growth of the gradients of the cosmogenic radionuclide production rates. Perhaps, the similar reasons are responsible for the currently observed sudden violations of the climate, which makes the necessity of studying the gradients of the cosmogenic radionuclide production rates especially urgent.

The progress achieved in the contemporary research of ordinary chondrites allows one to hope also to their further perspectiveness. The analytical

method of nuclear process description in cosmic bodies is verified in the unique experiment on isotropic irradiation of the rotating target of iron meteorite by the proton flux of the synchrocyclotron (Lavrukhina et al., 1973). Non-destructive low-level measurements of radionuclide contents are carried out by underground gamma-ray spectrometers, where the background reduction by the factor exceeding 10 could be achieved [Laubenstein, et al., 2004; Povinec, et al., 2005; 2015]. The excellent energy resolution and high detection efficiency of large volume HPGe detectors, which permit the selective and non-destructive analyses of several radionuclides in composite samples, are the main reasons why these detectors have been used (Alexeev, et al., 2015). Carrying out the monthly balloon measurements of the intensity of the primary component of GCRs with  $E \geq 100$  MeV (Stozhkov, et al., 2009), by which the cosmogenic radionuclides are produced at the depths of  $\geq 10$  cm from the surface, is critically important. The world-wide bolides network for meteorite fall photographing, providing the exact calculation of the meteorite orbits, is being developed. (Meier, 2016).

The perspectiveness and actuality of study of the gradients of the cosmogenic radionuclide production rates in the fresh-fallen chondrites (especially in connection with the current problems of the climate) makes it possible to put forward an effective draft of the global patrol surface for investigation of the GCR spatial and temporal variations in the heliosphere (Ustinova and Alexeev, 2018).

---

*The work is fulfilled within the topic of GEOKHI RAS.*

*I express my gratitude to T. A. Pavlova for the assistance in work.*

## References

- Alexeev V.A., et al. // *Adv. Space Res.* 2015. Vol. 56. P. 766-771. Doi: 10.1016/j.asr.2015.05.004
- Armstrong T.W. // *J. Geophys. Res.*, 1969, Vol.74, P. 1361-1373.
- Arnold J.R., Honda M., Lal D. // *J. Geophys. Res.* 1961. Vol. 66, P. 3519-3531.
- Bhandari N., et al. // *Nucl. Tracks.* 1980. Vol.4, P.213-262.
- Bhandari N., et al. // *Meteoritics.* 1994. Vol. 29, P. 443-444.
- Dorman L.I. *Cosmic Ray Variations and Space Research.* M. Nauka. 1963. 1027 p.
- Evans I.C. et al. // *J. Geophys. Res.* 1982. Vol. 87, P. 5577-5591.
- Kohman T.P. and Bender M.I. // *High-energy nuclear reactions in astrophysics.* N.Y. : Benjamin, 1967. P. 169-245.
- Lal D. // *Space Sci. Rev.*, 1972. Vol. 14, P. 3-102.
- Laubenstein, M., et al. // *Applied Radiation and Isotopes* . 2004. Vol. 61, P. 167-172.
- Lavrukhina A.K. *Nuclear reactions in cosmic bodies.* M.: Nauka. 1972. 254 p.
- Lavrukhina A.K. and Ustinova G.K. // *Astron. J.* (Russian).1967. V. 44, P. 1081-1086.
- Lavrukhina A.K. and Ustinova G.K. *Meteorites probes of cosmic ray variations.* (in Russian) M: Nauka. 1990. 264 p.
- Lavrukhina, et al. // *Atomic Energy.* 1973. Vol.34, P. 23-28.
- Lavrukhina A. K. and Ustinova G. K. // *Nature (London).* 1971. Vol. 232., P. 462-463; doi: 10.1038/232462a0
- Meier M.M.M. *Meteorites with photographic orbits.* 2016. <http://www.meteoriteorbits.info>
- Parker E. N. *Cosmic magnetic fields.* 1979. Oxford: Clarendon press. 841p.
- Povinec, P.P., Comanducci, J.F., Levy-Palomo, I // *J. Radioanalyt. Nucl. Chem.*. 2005. Vol. 263. P. 441-445.
- Povinec, P., et al. // *Meteoritics & Planetary Science.* 2015. Vol. 50. P.880.
- Potgieter M.S. // *Living Rev. Solar Phys.*.2013. Vol. 10. P. 3-66.
- Reedy R.C and Arnold J.K. // *J. Geophys. Res.* 1972. Vol. 77. P. 537-555.
- Stozhkov Yu.I. et al. // *Adv. Space Res.* 2009. Vol. 44. P. 1124-1137.
- Ustinova G.K. // *Dokl. Phys.* 2016. Vol. 61. No.11, P. 571-576.
- Ustinova G.K. and Alexeev V.A. // *Geochemistry International.* 2020. V. 58. No. 5. P. 487-499.
- Ustinova G.K. // *Experiment in Geosciences* 2018. Vol. 24, P. 51-55.
- Ustinova G.K. // *Analysis of the solar proton effects in the Stubenberg and Jesenice chondrites.* (iPosterSessions - an aMuze! Interactive system) at: The 52th Lunar and Planetary Science Conference, 2021. 1310.
- Ustinova G.K. and Alexeev V.A. // *Presentation at The 81<sup>st</sup> Ann. Meet. Met. Soc., Moscow, 2018;* DOI:10.13140/RG.2.2.29814.70726 (ID 8579); *Meteoritics and Planetary Science.* 2018. Vol. 53. S1-6056.
- Ustinova G.K. and Lavrukhina A.K., // *Proc. 21st Intern. Cosmic Ray Conf., 1990, Adelaide. Vol. 7, P. 141-144.*

### Kuyunko N.S. The thermoluminescent researches of equilibrium ordinary chondrites of shock classes S1-S3 UDC 550.42

Vernadsky Institute of Geochemistry and Analytical Chemistry RAS, Moscow (ninakuyunko@gmail.com)

**Abstract.** The results of researches of equilibrium ordinary chondrites of shock classes S1-S3 by the thermoluminescent method are presented. Measurements of natural (accumulated in outer space) and laboratory-induced thermoluminescence of meteorites from an external radioactive radiation source in the temperature range of 50-350°C. The thermoluminescence intensity was calculated relative to the Dhajala H3.8 chondrite. The temperatures of the maximum peak of the thermoluminescent glow, its height and the area under the glow curve of the studied meteorites were determined. Comparative measurements of natural and gamma-induced thermoluminescence and calculation of the equivalent radiation dose allowed us to estimate the magnitude of the perihelion of the orbit of the studied chondrites. The results are consistent with the data obtained by other methods.

**Keywords:** *thermoluminescence, ordinary chondrites, shock metamorphism, perihelion.*

Meteorites at the stage of existence of independent cosmic bodies retain information about cosmic rays irradiation and collisions during their evolution. Under the influence of cosmic radiation, in addition to cosmogenic isotopes, traces of radiation disturbances accumulate in the mineral components of meteorites, which cause thermoluminescent glow when the substance is heated. The thermoluminescent method is successfully used to study the impact-thermal history of meteorites, estimate orbits, Earth ages, etc. Periodic changes in the perihelion of chondrites during  $\sim 10^7$  years can lead to diffusive loss of gases at perihelion  $\leq 0.2$  au (heating temperature  $T \geq 400$  °C) and over-accumulation of natural thermoluminescence at perihelion  $\sim 1$  au during the last  $\sim 10^5$  years before capture by the Earth.

Induced thermoluminescence (TLind) (induced in laboratory conditions from an external radioactive radiation source) is used to study shock metamorphism. Natural thermoluminescence (TLnat) accumulated in outer space reflects the history of meteorite irradiation by galactic cosmic rays and thermal heating by the Sun depending on the proximity of the location (Sears, 1988). The closer the meteorite approaches the Sun (perihelion), the higher the temperature of its heating and, consequently, the more the accumulated natural thermoluminescence runs out. The amount of natural

---

thermoluminescence remaining determines the value of the equivalent dose, which is easily measured when irradiating a meteorite sample under laboratory conditions. The time spent by the meteorite at the maximum distance from the Sun (aphelion) at the minimum heating temperature is reflected in the results of measurements of natural thermoluminescence by the amount of saturation dose. This value is determined by repeated irradiation of the sample under laboratory conditions from an external source with different radiation doses.

Determining the parameters of meteorite orbits is possible if the amount of natural thermoluminescence accumulated by a meteorite in outer space has reached the equilibrium stage. This stage occurs provided that the meteorite has been isolated from the parent body and has been irradiated by cosmic rays for more than  $10^5$  years. In the work (Sears, 1988) it is shown that all fallen meteorites satisfy this condition. A strong collision of meteorites in outer space leads to a significant decrease in the level of accumulated natural thermoluminescence. Therefore, we selected chondrites from the collection of meteorites of the GEOCHI RAS of shock classes S1-S3. It should be noted that the amount of accumulated natural thermoluminescence varies with the depth of the test sample, which should require making appropriate adjustments to the measurement results. However, in the work (Melcher, 1981) it was shown that the change in the intensity of thermoluminescence with the depth of the sample does not exceed 30%. To estimate the parameters of meteorite orbits, this value is not significant and it can be ignored.

For the study, gross samples of meteorites weighing 0.7-1.0 g were crushed and crushed in a jasper mortar under a layer of ethyl alcohol. After drying for a day in the air, the magnetic fraction was separated with a hand magnet. Three samples weighing 2 mg were prepared from the non-magnetic fraction of each sample under study by quartering. Each sample was placed in a beryllium foil cup with a diameter of 6 mm and evenly distributed along the bottom with a drop of acetone under a binocular. The solvent was removed by air drying during the day. Thermoluminescence was recorded on a modified laboratory setup. The interface made on the basis of the L-154 board made it possible to register the photomultiplier current and the heating temperature of the sample on the computer. The discreteness of registration was  $1^\circ\text{C}$ . After measuring the natural thermoluminescence, the samples were irradiated with X-ray and gamma radiation from an external  $^{137}\text{Cs}$  radioactive source under laboratory conditions. The thermoluminescence parameters were calculated relative to Dhajala H3.8 chondrite. The average value of three measurements was used. The results of

thermoluminescent measurements are shown in the figure and in the table.

As noted above, thermoluminescence accumulated in outer space reaches equilibrium over a period of approximately  $10^5$  years. Changing the parameters of the meteorite's orbit should lead to a change in the level of natural thermoluminescence. After the meteorite falls to Earth (due to the actual cessation of irradiation by galactic cosmic rays), the level of natural thermoluminescence accumulated in the high-temperature region of the luminescence spectrum (more than  $200^\circ\text{C}$ ) remains constant if the meteorite has not been subjected to prolonged heating to a temperature close to  $100^\circ\text{C}$ . The heating of a meteorite during its passage through the Earth's atmosphere covers an area less than 5 mm deep from the outer surface. Careful sampling without the melting crust of the meteorite makes it possible to exclude a possible underestimation of the level of natural thermoluminescence.

In most ordinary chondrites, the levels of natural thermoluminescence are observed in the range of 200-1800 Gy (Melcher, 1981, Bronshten, 1999). The calculation of the value of natural thermoluminescence in ordinary chondrites suggests that the intensity of thermoluminescence is a sensitive indicator of the degree of their heating by the Sun, depending on the perihelion. Chondrites having orbits with a perihelion less than 0.85 au should show very low levels of natural thermoluminescence (less than 50 Gy for a temperature of  $\sim 250^\circ\text{C}$  on the glow curve). At the same time, orbits with a perihelion greater than 0.85 au should show a wide range of natural thermoluminescence (more than 50 Gy) with significant dispersion associated with variations in the amount of accumulated dose, which may depend on the depth of the sample and albedo (Melcher, 1981). However, a direct comparison of the thermal and radiation history of meteorites solely on the basis of natural thermoluminescence is impossible due to significant variations in the sensitivity of induced thermoluminescence in various meteorites. Therefore, it is necessary to normalize the intensity of natural thermoluminescence in each sample to its sensitivity by measuring the amount of induced thermoluminescence per unit of radiation dose (D) from a radioactive source. The ratio value, known as the equivalent dose (ED), is determined for a given temperature on the glow curve and calculated by the formula:  $ED = D (TL_{nat}/TL_{ind})$ , where  $TL_{nat}$  and  $TL_{ind}$  are the values of natural and induced thermoluminescence, respectively, D is the dose value (G) induced in laboratory conditions (Melcher, 1981, Benoit et al., 1991).

TL

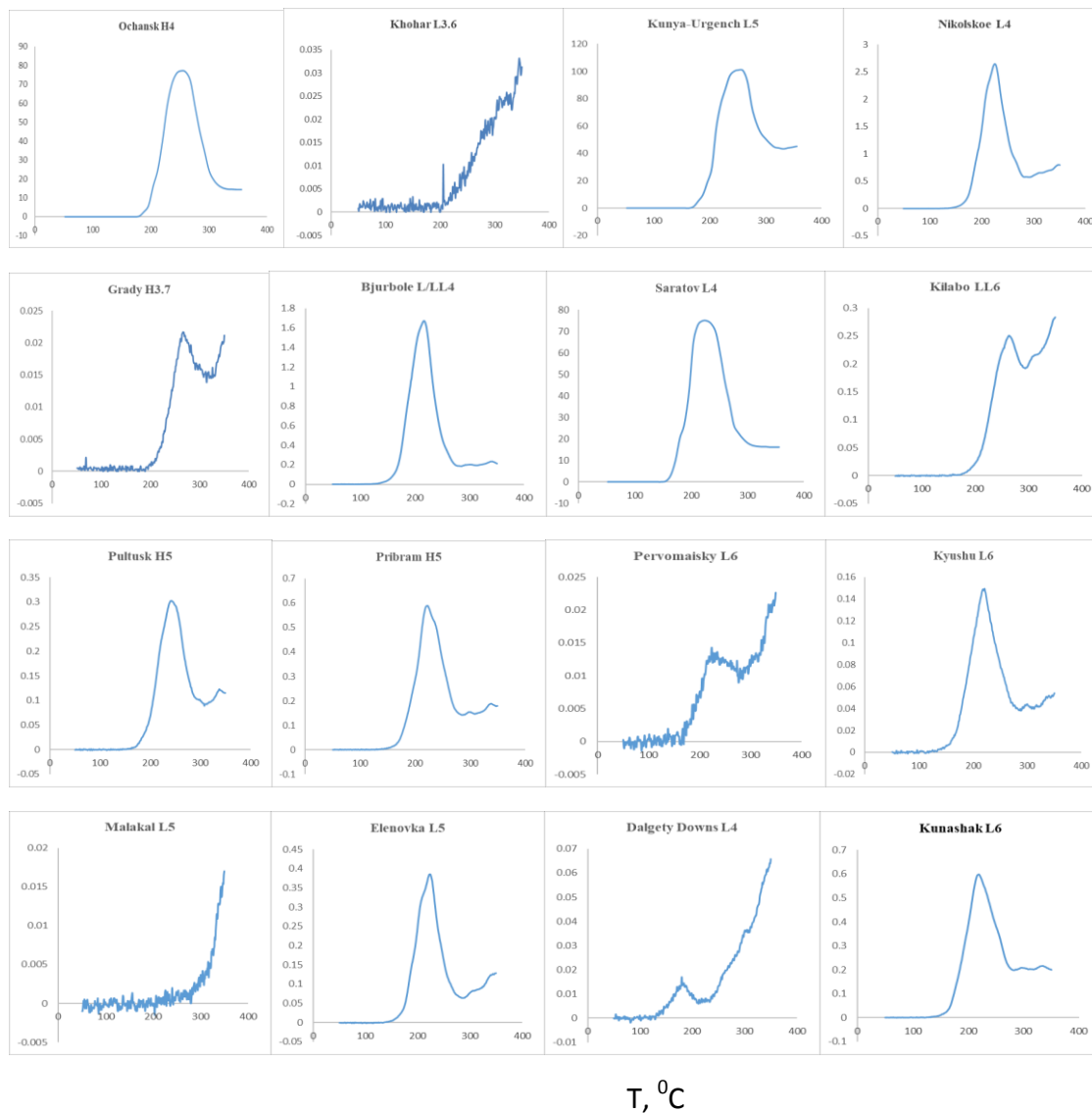


**Fig.** Spectra of natural thermoluminescence of ordinary chondrites.

In our calculations, we calculated the value of ED not for a given temperature, but for the temperature range on the glow curves 100-240°C – ED<sub>low</sub> and 240-340°C – ED<sub>high</sub>. This made it possible to determine the value of the equivalent dose with an error of less than 15% and to more accurately estimate the magnitude of the perihelion. The calculated values of ED<sub>low</sub> and ED<sub>high</sub> based on the results of comparative measurements of natural and gamma-induced thermoluminescence are shown in the table. The ED values for most of the chondrites studied in this work correspond to a perihelion of ~1.0-0.8 au, a smaller perihelion value was determined only for Malakal chondrite ~0.5-0.6 au, which is consistent with the results (Melcher, 1981, Benoit et al., 1991). The perihelion value of ~1 au for

the Kunya-Urgench orbit is consistent with the estimate calculated from the incident chondrite radiant (Bronshen, 1999).

**Conclusions.** Measurements of natural and laboratory-induced thermoluminescence from an external radioactive radiation source of ordinary equilibrium chondrites in the temperature range of 50-350°C were performed. The temperatures of the maximum peak of the thermoluminescent glow, its height and the area under the glow curve are determined. Comparative measurements of natural and gamma-induced thermoluminescence and calculation of the equivalent radiation dose allowed us to estimate the magnitude of the perihelion of the orbit of the studied chondrites.

**Tabl.** Parameters of thermoluminescent studies of ordinary chondrites.

No.	Meteorite	Type	TLnat	TLind	EDlow	EDhigh
1	Dhajala	H3.8			17	210
2	Pribram	H5	2.931	1.058	114	1270
3	Saratov	L4	52.676	1.579	171	560
4	Bjurbole	L/LL4	6.83	1.303	380	1560
5	Elenovka	L5	1.873	2.478	39	230
6	Nikolskoe	L4	13.188	3.492	161	1590
7	Kunashak	L6	3.45	1.572	166	432
8	Pultusk	H5	1.61	1.017	46	810
9	Ochansk	H4	47.58	1.019	107	1050
10	Kohar	L3.6	0.153	0.189	12	513
11	Malakal	L5	0.03	0.288	12	24
12	Kunya-Urgench	L5	79.509	4.913	112	1000
13	Kyushu	L6	0.805	0.153	300	1810
14	Pervomaisky	L6	0.132	0.028	201	710
15	Dalgety Downs	L4	0.286	0.525	2	300
16	Grady	H3.7	0.446	0.528	14	800
17	Kilabo	LL6	1.864	2.184	35	510

*The work was carried out within the framework of the budget topic of the Vernadsky Institute of Geochemistry and Analytical Chemistry of the Russian Academy of Sciences.*

#### References

1. Benoit P.H., Sears D.W.G., McKeever S.W.S. (1991) The natural thermoluminescence of meteorites. II. Meteorite orbits and orbital evolution. *Icarus*. V.94. No. 2. P.311-325.
2. Melcher S.L. (1981) Thermoluminescence of meteorites and their terrestrial age. *Geochim. Cosmochim. Acta*. V.45. P.615-626.
3. Melcher S.L. (1981) Thermoluminescence of meteorites and their orbits. *Earth Planet. Sci. Lett.* V.2. No. 1. P. 39-54.
4. Sears D.W.G. (1988) Thermoluminescence of meteorites: Shedding light on the cosmos. *Nucl.Tracks. Radiat. Meas.* V.14. No. 1/2. P.5-17.
5. Bronshten V.A. (1999) Astronomical conditions of the fall and orbit of the Kunya-Urgench meteorite. *Letters to the Astronomer. Journal.* Vol.25. No. 2. P.153-155.